Design of tunable shunt rainbow trap smart beam for multi-frequency vibration attenuation

Matheus C. R. Borges[1], Braion B. Moura[1], Marcela R. Machado[1]

[1]*Department of Mechanical Engineering, University of Brasília, Brasília, DF, Brazil*
Campus Universitário Darcy Ribeiro, Asa Norte, Brasília-DF, CEP 70910-900
Canedo001@gmail.com, braionbarbosa@gmail.com, mromarcela@gmail.com

Abstract. This paper analyzes a strategy for tunable, broadband vibration attenuation in electro mechanics alone-dimension guided wave coupled with shunted piezoelectric. The piezo patches are in periodic arrays over the beam. They are connected in shunt circuits that resonate at distinct neighbouring frequencies, creating a tunable rainbow trap capable of attenuating vibration with broadband characteristics. Based on the effect of electrical energy dissipation, the shunt circuit connection is applied to provide damping in the system vibration. An efficient method to model and analyze the dynamic of structures is the spectral elements method (SEM). Although, a single spectral element can model geometrically uniform members. Therefore, it can reduce the total number significantly in the mesh. Results show the efficiency in attenuating vibrations over a broad frequency range can be obtained by tuning different shunt circuits to resonate at different frequencies, which create a tunable rainbow trap.

Keywords: Smart beam, Vibration control, Piezoelectric, Resonant Shunt, Rainbow Trap.

1 Introduction

Control and attenuation of vibrations is an important issue, and it is receiving more and more attention over the past years. Using piezoelectric shunts, a passive technique for vibration control of flexible structures has grown its application in vibration attenuation and control. In the passive control technique, the only external element to be used is a passive electrical network that is directly connected to the electrodes of the piezoelectric circuit [11]. This technique was first introduced by Forward [6] who used piezoelectric elements with inductive shunts to reduce the wave propagation of a membrane mirror [2].

Since the piezoelectric material can convert mechanical energy into electrical energy and vice versa, the shunt circuit known to dissipate this energy is largely applied on wave attenuation and vibration control [10]. The resistive inductive (RL) circuits can generate localized vibration attenuation. By connecting an RL circuit with a capacitor and it is obtained a resonant RLC circuit, which behaves as an electrical dynamic damper that can be tuned by adjusting the circuit parameters [3, 9,10]. Hagood and Von Flotow [2] contributed to the first analytical formulation for passive shunt implementation, demonstrating how a piezoelectric patch shunted through a resistive inductive (RL) circuit acts as a vibration absorber when adjusted for the resonance frequency of the structure. Airoldi and Ruzzene [1] implemented a periodic structure with independent RL shunt circuits to control wave propagation, this work demonstrated promising results in terms of locally resonant bandgap generation. Cardella et al.[15] presented the piezo patch configuration capable of attenuating vibrations over a broad frequency range can be obtained by tuning different RL circuits to resonate at different frequencies, thus realizing a tunable rainbow trap for elastic wave manipulation.

Regarding the idea proposed by Cardella et al.[15], this paper discusses the development of an SEM numerical model of a unimorph beam structure, represented by a beam coupled with a piezo layer, aiming to study the tunable rainbow trap configuration used to manipulate the vibration attenuation. Numerical results used the rainbow trap technique using an RLC shunt circuit to achieve efficiency in attenuating vibrations over a broad frequency range. The general impedance relationships of the circuit give the interactions between the structure and the shunt circuit. Results show the efficiency of the technique and the rainbow kind attenuation in the beam's vibration.

2 Spectral Element Theoretical Analysis

Dynamic models of smart structures connected with circuits shunts are developed based on Modal Analysis (MA), Finite Element Method (FEM), Wave Finite Element (WFE), among other techniques[8]. However, these methods require a certain mathematical complexity, and some need a large number of discretization's expressing precision in the system's responses. The Spectral Element Method (SEM) is an alternative to other methods since its formulation deals with a model that relates forces and displacements spectral nodal based on the analytical solution of the wave [4,7]. Therefore, SEM does not need a discretization with large numbers of elements. The smart beam structure model of Fig. 1 used the piezo patched couplings in a periodical order.

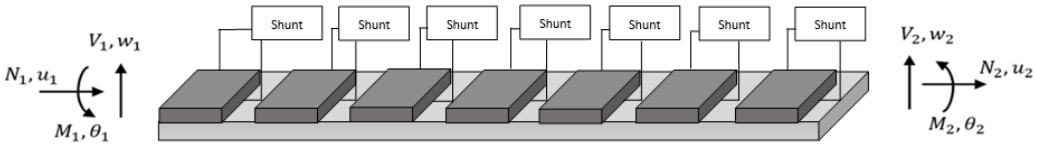

Figure 1. Smart material beam.

The smart beam represented in Figure 1 is composed of joints of elements of the type beam-piezo-shunt and beam also called unimorph beam. The structure presents homogeneous density and thickness, perfect continuity at the interfaces, small vibration amplitudes and linear elasticity. The variables of transverse displacement, axial displacement and rotation are represented by the terms $w(x,t)$, $u(x,t)$ and $\theta(x,t)$. The relations of bending moments, shear force and axial force are represented by M, V and N.

2.1 Spectral Element Modeling of the beam metamaterial with shunted circuit

The beams are structural elements that have the dimension of the cross-section less than the total length. The mathematical model for the Euler-Bernoulli beam considering the dimensions uniform prismatic has the following equation of motion,

$$EI\ \frac{\partial^4 w(x,t)}{\partial x^4} = \rho A \frac{\partial^2 \theta(x,t)}{\partial t^2} + f(x,t) \tag{1}$$

where E, ρ, A and I are Young's modulus, mass density, transverse area and moment of inertia, respectively. Assuming that the transverse displacement and rotation can be expressed as

$$\begin{Bmatrix} w(x,t) \\ \theta(x,t) \end{Bmatrix} = \frac{1}{N} \sum_{n=0}^{N-1} \begin{Bmatrix} W(x,\omega_n) \\ \Theta(x,\omega_n) \end{Bmatrix} e^{i\omega_n t} \tag{2}$$

By considering the external force $f(x,t) = 0$ and applying the spectral terms of Eq. (2) in Eq. (1), we obtained the equation of motion of the beam in the frequency domain, expressed by

$$EI\ \frac{\partial^4 W(x,\omega_n)}{\partial x^4} - \omega^2 \rho A W(x,\omega_n) = 0 \tag{3}$$

The general solution is assumed of type $W = ae^{-ik(\omega)x}$ and its solution represents the following dispersion relation $k^4 - k_F^4 = 0$, where k_F does the following relation define the wavenumber as

$$k_F = \sqrt{\omega} \left(\frac{\rho A}{EI}\right)^{1/4} \tag{4}$$

Therefore, the general solution under wave propagation base is

$$w = a_1 e^{-ik_F x} + a_2 e^{-k_F x} + a_3 e^{ik_F x} + a_4 e^{k_F x} = \boldsymbol{e}(x,\omega)\boldsymbol{a} \tag{5}$$

where $\boldsymbol{e}(x,\omega) = [e^{-ik_F x},\ e^{-k_F x},\ e^{ik_F x},\ e^{k_F x}]$, and $\boldsymbol{a} = \{a_1,\ a_2,\ a_3,\ a_4\}^{\boldsymbol{T}}$. For finite beam element of length L with defined nodes on the contours $x = 0$ and $x = L$, we have that the transverse displacement and rotation can be related to the wave equation,

$$\boldsymbol{d} = \begin{Bmatrix} W_1 \\ \Theta_1 \\ W_2 \\ \Theta_2 \end{Bmatrix} = \begin{Bmatrix} \boldsymbol{e}(0,\omega) \\ \boldsymbol{e}'(0,\omega) \\ \boldsymbol{e}(L,\omega) \\ \boldsymbol{e}'(L,\omega) \end{Bmatrix} = \boldsymbol{H}_B(\omega)\boldsymbol{a}, \tag{6}$$

where $\boldsymbol{H}_B(\omega) = \begin{bmatrix} 1 & 1 & 1 & 1 \\ -ik_F & -k_F & ik_F & k_F \\ e^{-ik_F L} & e^{-k_F L} & e^{ik_F L} & e^{k_F L} \\ -ik_F e^{-ik_F L} & -k_F e^{-k_F L} & ik_F e^{ik_F L} & k_F e^{k_F L} \end{bmatrix}$,

One can express the components of force and moment as

$$\boldsymbol{f_c} = \begin{Bmatrix} Q_1 \\ M_1 \\ Q_2 \\ M_2 \end{Bmatrix} = \begin{Bmatrix} -Q(0) \\ -M(0) \\ Q(L) \\ M(L) \end{Bmatrix} = \boldsymbol{G}_B(\omega)\boldsymbol{a}, \tag{7}$$

where $(x) = -EIW'''(x),\ M(x) = EIW''(x)$, and

$$\boldsymbol{G}_B(\omega) = \begin{bmatrix} -ik_F^3 & ik_F^3 & k_F^3 & -k_F^3 \\ -ik_F^2 & ik_F^2 & k_F^2 & -k_F^2 \\ ik_F^3 e^{-ik_F L} & -ik_F^3 e^{ik_F L} & -k_F^3 e^{k_F L} & k_F^3 e^{-k_F L} \\ k_F^2 e^{-ik_F L} & -k_F^2 e^{ik_F L} & ik_F^2 e^{k_F L} & -ik_F^2 e^{-k_F L} \end{bmatrix},$$

By relating Eq. (6) with Eq. (7), it is possible to establish the relations between displacement and force,

$$\boldsymbol{S}_B(\omega) = \boldsymbol{G}_B(\omega)\boldsymbol{H}_B^{-1}(\omega), \tag{8}$$

where $\boldsymbol{S}_B(\omega)$ is the dynamic stiffness matrix, also known as the spectral stiffness matrix for the Euler-Bernoulli beam.

2.2 Spectral Element analysis of the Beam-piezo element

The linear constitutive relationships used to represent electromechanical behaviour one-dimension of the piezoelectric material are expressed with,

$$\begin{Bmatrix} \sigma \\ E_c \end{Bmatrix} = \begin{bmatrix} C_{11}^D & -h_{31} \\ -h_{31} & \beta_{33}^S \end{bmatrix} \begin{Bmatrix} \epsilon \\ D_3 \end{Bmatrix}, \tag{9}$$

where σ is the mechanical stress, ϵ the mechanical strain, D_3 is the electrical displacement (charge/area in the vertical beam direction), β_{33}^S the dielectric constant, C_{11}^D is the elastic modulus, E_c is the dielectric constant, and h_{31} is the piezoelectric constant. The formulation of the spectral element starts with the exact solution of the equation of the motion. Therefore, to build the motion equation of a piezo coupled beam element, Lee [7] uses the relations of kinetic energy, potential and virtual work to apply Hamilton's principle and generate the following motion of equation,

$$\begin{gathered} EIw'''' + \rho A\ddot{w} + cA\dot{w} = -\alpha\ddot{u}_b' + \beta u''' + \gamma\ddot{w}'' + c_1\dot{w}'' - c_4\dot{u}_b' + Fw'' + p(x,t) \\ EAu_b'' - \rho A\ddot{u}_b - cA\dot{u}_b = -\alpha\ddot{w}' + \beta w''' - c_4\dot{w}' - \tau(x,t), \end{gathered} \tag{10}$$

$$\begin{aligned} EA &= E_bA_b + E_pA_p, & EI &= E_bI_b + E_pI_p + (1/4)E_pA_ph^2, & c_1 &= (1/4)c_pA_ph^2, \\ \rho A &= \rho_bA_b + \rho_pA_p, & \alpha &= (1/2)\rho_pA_ph, & c_4 &= (1/2)c_pA_ph, \\ \beta &= (1/2)E_pA_ph, & \gamma &= (1/4)\rho_pA_ph^2, & cA &= c_bA_b + c_pA_p, \end{aligned}$$

where subscripts b e p represent the beam and piezo elements, respectively. The terms E, ρ, c, A and I are Young's modulus, mass density, viscous damping coefficient, transverse area and moment of inertia, respectively. The sum of the thicknesses of the beam and the piezo is represented by h; F is the constant axial tensile force, $p(x,t)$ and $\tau(x,t)$ are possible external forces applied along the beam. For simplification of notation, spatial partial derivatives

are represented by ($'$), while partial time derivatives are characterized by ($\dot{}$). The structural damping of each element can be readily taken into account using the complex modulus of elasticity as $E_b^* = E_b(1 + i\eta_b)$, $E_p^* = C_{11}^{D*} - h_{31}^2\beta_{33}^{S-1}$, $C_{11}^{D*} = C_{11}^{D}(1 + i\eta_p)$. The following spectral forms are assumed

$$\begin{Bmatrix} w(x,t) \\ u(x,t) \\ p(x,t) \\ \tau(x,t) \end{Bmatrix} = \frac{1}{N}\sum_{n=0}^{N-1} \begin{Bmatrix} W(x,\omega_n) \\ U(x,\omega_n) \\ P(x,\omega_n) \\ T(x,\omega_n) \end{Bmatrix} \tag{11}$$

By applying the spectral terms of Eq. (11) in Eq. (10), we obtained the equation of motion in the frequency domain, expressed by

$$\begin{gathered} EIW'''' - \omega^2\rho AW + i\omega cAW = \omega^2\alpha U' + \beta U''' - \omega^2\gamma W'' + i\omega c_1 W'' - i\omega c_4 U' + FW'' + P(x) \\ EAU'' + \omega^2\rho AU - i\omega cAU = \omega^2\alpha W' + \beta W''' - i\omega c_4 W' - T(x), \end{gathered} \tag{12}$$

The general solution is assumed of type $W(x) = \sum_{i=1}^{6}(a_j e^{-ik_j x}) = \boldsymbol{e}(x,\omega)\boldsymbol{a}$, $U(x) = \sum_{i=1}^{6}(r_j a_j e^{-ik_j x}) = \boldsymbol{e}(x,\omega)\boldsymbol{Ra}$, where $\boldsymbol{e}(x,\omega) = [e^{-ik_1x}\ \ e^{-ik_2x}\ \ e^{-ik_3x}\ \ e^{-ik_4x}\ \ e^{-ik_5x}\ \ e^{-ik_6x}]$, $\boldsymbol{a} = \{a_1\ \ a_2\ \ a_3\ \ a_4\ \ a_5\ \ a_6\}^T$, and

$$\boldsymbol{R} = diag(r_j) = diag\left[\frac{-\omega k_j c_4 - i\omega^{2k_j}\alpha + ik_j^3\beta}{-k_j^2 EA + \omega^2\rho A - i\omega cA}\right]$$

From the general solution applied to the equation of motion, a characteristic equation with an eigenvalue problem is obtained, and the wavenumbers k_j $(j = 1,2..,6)$ are determined by estimating the roots of the following expression

$$b_1 k^6 + b_2 k^4 + b_3 k^2 + b_4 = 0, \tag{13}$$

$$\begin{gathered} b_1 = \beta^2 - EAEI, \\ b_2 = \omega^2(EA\gamma + EI\rho A - 2\alpha\beta) - i\omega(EIcA + EAc_1 - 2\beta c_4) - EAF, \\ b_3 = \omega^4(\alpha^2 - \gamma\rho A) + i\omega^3(\rho Ac_1 + \gamma cA - 2\alpha c_4) + \omega^2(EA\rho A + cAc_1 + F\rho A - c_4^2) - i\omega cA(EA + F), \\ b_4 = -\rho A^2\omega^4 + 2i\omega^3\rho AcA + \omega^2 cA^2. \end{gathered}$$

Relating the spectral nodal shifts in terms of $\boldsymbol{a}$ with the vector $\boldsymbol{d}$, we obtain $\boldsymbol{d} = \boldsymbol{H}_{BP}(\omega)\boldsymbol{a}$, where

$$\boldsymbol{H}_{BP}(\omega) = \begin{bmatrix} r_1 & r_2 & r_3 & r_4 & r_5 & r_6 \\ 1 & 1 & 1 & 1 & 1 & 1 \\ -ik_1 & -ik_2 & -ik_3 & -ik_4 & -ik_5 & -ik_6 \\ e^{-ik_1L}r_1 & e^{-ik_2L}r_2 & e^{-ik_3L}r_3 & e^{-ik_4L}r_4 & e^{-ik_5L}r_5 & e^{-ik_6L}r_6 \\ e^{-ik_1L} & e^{-ik_2L} & e^{-ik_3L} & e^{-ik_4L} & e^{-ik_5L} & e^{-ik_6L} \\ -ik_1e^{-ik_1L} & -ik_2e^{-ik_2L} & -ik_3e^{-ik_3L} & -ik_4e^{-ik_4L} & -ik_5e^{-ik_5L} & -ik_6e^{-ik_6L} \end{bmatrix},$$

Assuming general solutions of the type $W(x,\omega) = \boldsymbol{N}_w(x,\omega)\boldsymbol{H}_{BP}^{-1}(\omega)$, $U(x,\omega) = \boldsymbol{N}_u(x,\omega)\boldsymbol{d}$, where the shape functions are given by $\boldsymbol{N}_w(x,\omega) = \boldsymbol{e}(x,\omega)\boldsymbol{H}_{BP}^{-1}(\omega)$, $\boldsymbol{N}_u(x,\omega) = \boldsymbol{e}(x,\omega)\boldsymbol{R}\boldsymbol{H}_{BP}^{-1}(\omega)$. Relating the general solution to the equation of motion and applying Hamilton's principle, we arrive at the following spectral element equation

$$\boldsymbol{S}_{BP}(\omega)\boldsymbol{d} = \boldsymbol{f}(\omega), \tag{14}$$

and replacing the dynamic shape functions into Eq. (14) gives

$$\boldsymbol{S}_{BP}(\omega) = \boldsymbol{H}_{BP}^{-T}(\omega)\boldsymbol{D}(\omega)\boldsymbol{H}_{BP}^{-1}(\omega), \tag{15}$$

where

$$\begin{gathered} \boldsymbol{D}(\omega) = -EA\boldsymbol{RKEKR} + EI\boldsymbol{K^2EK^2} - i\beta(\boldsymbol{K^2EKR} + \boldsymbol{RKEK^2}) - \omega^2[\rho A(\boldsymbol{E} + \boldsymbol{RER}) + \\ i\alpha(\boldsymbol{KER} + \boldsymbol{REK}) - \gamma KEK] + i\omega[cA(\boldsymbol{E} + \boldsymbol{RER}) - c_1\boldsymbol{KEK} + ic_4(\boldsymbol{KER} + \boldsymbol{REK})] - F\boldsymbol{RER}, \end{gathered}$$

with $\boldsymbol{K} = diag[k_j]$, $\boldsymbol{K^2} = diag[k_j^2]$, $\boldsymbol{E}(\omega) = \int_0^L \boldsymbol{e}^T(x,\omega)\boldsymbol{e}(x,\omega)dx$,

2.3 Spectral element of shunt control

The mathematical representation of connecting an electrical shunt circuit to a piezoelectric represents the energy relation with mechanical deformation. The equation of beam-piezo movement with electrical shunt circuit is given by

$$\begin{gathered} EIw'''' + \rho A\ddot{w} + cA\dot{w} + \Gamma V = -\alpha\ddot{u}_b' + \beta u''' + \gamma\ddot{w}'' + c_1\dot{w}'' - c_4\dot{u}_b' + Fw'' + p(x,t) \\ EAu_b'' - \rho A\ddot{u}_b - cA\dot{u}_b + \Gamma V = -\alpha\ddot{w}' + \beta w''' - c_4\dot{w}' - \tau(x,t), \\ E\Gamma\dot{v} + C_p^T\dot{V} = I, \end{gathered} \tag{16}$$

where I is current, V is the voltage, C_p^T is the piezoelectric capacitance, Γ is the coupling term, defined by the following relationships

$$V = -Z_{eq}I, \qquad C_p^T = A(C_{11}^D - h_{31}^2/\beta_{33}^S), \qquad \Gamma = A(C_{11}^D - h_{31}^2/\beta_{33}^S)/l \tag{17}$$

where Z_{eq} is the electrical impedance of the shunt circuit. The resonant type electrical shunt circuit with resistance and inductance connected in series, the following impedance is generated

$$Z_{eq} = \frac{R + i\omega L}{\left(1 - \omega^2 LC_p^T\right) + i\omega RC_p^T} \tag{18}$$

Equation (16) can be particularized to a harmonic motion and converted to the frequency domain. Thus, the corresponding harmonic motion assumption for generalized force and current is given by

e

$$\begin{aligned} \boldsymbol{S}_{BP}(\omega)\boldsymbol{d} - \boldsymbol{S}_{SH}(\omega)V(\omega) &= \boldsymbol{f}(\omega), \\ i\omega\boldsymbol{S}_{SH}(\omega)\boldsymbol{d} + i\omega\, C_p V(\omega) &= I(\omega), \end{aligned} \tag{19}$$

Rearranging the equation of motion in terms of the piezo-beam and shunt circuit spectral element matrices, one can obtain

$$[\boldsymbol{S}_{BP}(\omega) + \boldsymbol{S}_{SH}(\omega)]\boldsymbol{d} = \boldsymbol{f}(\omega), \tag{20}$$

where $\boldsymbol{S}_{sh}(\omega) = [\boldsymbol{N}_e(x_0,\omega) \quad 0 \quad -\boldsymbol{M}_e(x_0,\omega) \quad -\boldsymbol{N}_e(x_0,\omega) \quad 0 \quad \boldsymbol{M}_e(x_0,\omega)]^T$,

$$\boldsymbol{N}_e = \frac{k_{31}^2 i\omega Z_{eq} b d_{31} E_p}{1 + i\omega C_p^T Z_{eq}}, \qquad \boldsymbol{M}_e = \frac{k_{31}^2 i\omega Z_{eq} h b d_{31} E_p}{2 + 2i\omega C_p^T Z_{eq}}$$

Once the matrices of the spectral elements $\boldsymbol{S}_B(\omega)$, $\boldsymbol{S}_{BP}(\omega)$ and $\boldsymbol{S}_{SH}(\omega)$ are defined, it is possible to obtain the global matrix by assembling the elements. This procedure is similar to the one used in the Finite Element Method. Therefore, the global matrix can be written so that $\boldsymbol{S}_g(\omega)\boldsymbol{d}_g(\omega) = \boldsymbol{f}_g(\omega)$, where the subscript g indicates the global components.

3 Numerical analysis

The properties and geometries for the beam and the piezoelectric layer followed the work presented by [12,13,14]. The values are Young's modulus of $E_b = 71$ GPa, the density of $\rho_b = 2700$ kg/m^3, the width of $b_b = 12.7$ mm, and a thickness of $h_b = 2.286$ mm. The piezo material and geometrical properties are Young's modulus of $E_p = 64.9$ GPa, the density of $\rho_p = 7600\ kg/m^3$, width of $b_p = 12.7$ mm, and thickness of $h_p = 0.762$ mm. Piezoelectric constant is $d_{31} = -175\ m/V \times 10^{-12}$, the dielectric constant of $\beta_{33}^S = -350\ m/V \times 10^{-12}$, coupling coefficient $k_{31} = 0.31$, and stiffness of $C_p^T = 200\ GPa$. The total length of the smart structure is $L_s = 0.261$ m. The simulation was performed in MATLAB software, presenting a series resistive-inductive shunt circuit configuration with values of resistance $R = 33\ \Omega$ and inductance $L = 0.1516\ H$.

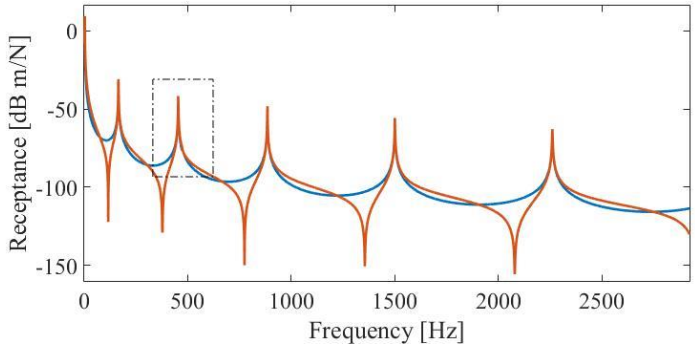

Figure 2. Receptance response of the beam in short-circuited obtained at both beam ends.

Figure 2 shows the receptance response of the beam in short-circuited obtained at both beam's ends due to a unitary force applied at the left-hand-side beam edge. For the rainbow circuit configuration, seven frequencies are chosen between 340Hz and 580Hz and each shunt circuit is connected to the piezo sensors tuned at a specific frequency. The colours of a rainbow represent each tuned frequency so that the RED (R) is the tunned frequency at $f = 400\ Hz$, the ORANGE (O) at $f = 425\ Hz$, the YELLOW (Y) at $f = 450\ Hz$, the GREEN (G) at $f = 475\ Hz$, the BLUE (B) at $f = 500\ Hz$, the NAVY (N) at $f = 525\ Hz$ and the VIOLET (V) at $f = 550\ Hz$.

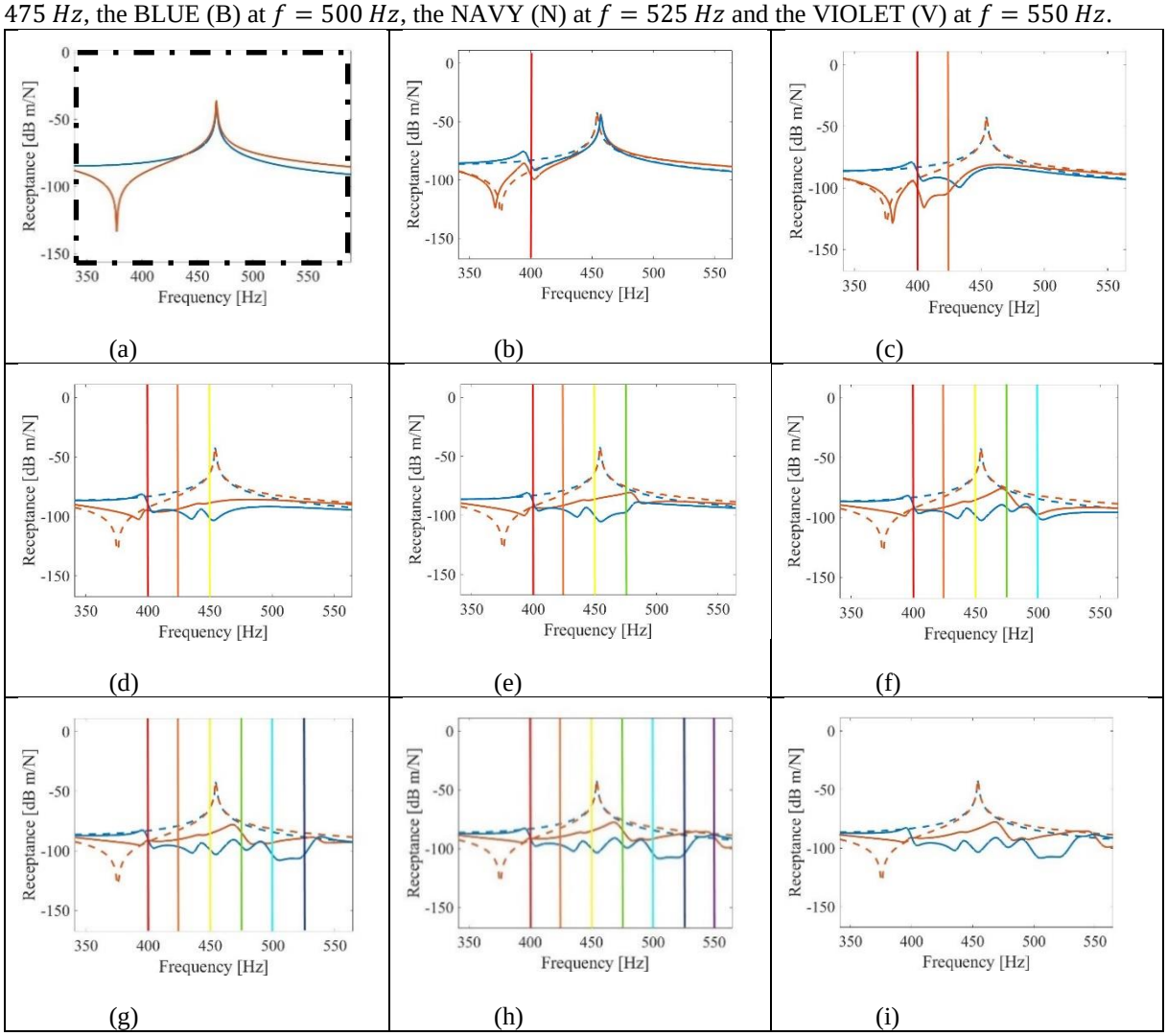

Figure 3. Rainbow technique implementation in the FRF response second mode shape: (a) Zoom view of the second resonance in the short-circuited configuration; (b)-(h) Zoom view of the second resonance after activating each shunt (ROYGBNV) sequentially; (i) final spectrum broadband attenuation obtained when all shunts are active in solid line compared to the short-circuited configuration in dashed line.

Figure 3(a) shows a zoon view of the receptance FRF response in the short-circuiting configuration in a frequency range of 350 to 560 Hz In this configuration the beam are resonating without control. Figure 3(b-h) shows the FRF zoom within each circuit shunt (ROYGBNV) in action one by one as illustrated by the colour lines. The vertical lines indicate the tuned resonant frequencies of each shunt circuit to operate. As we advance in the sequence of activation of the circuits the shunted patches progressively dissipated the vibration in that frequency range, until all shunts are activated and it achieved the maximum energy dissipation. Figure 3(i) allows visualizing fully the broadband vibration attenuation capability of the rainbow trap configuration.

4 Conclusions

In this article, we explore the functionality of the rainbow trap usage in control and attenuation of vibration in a beam using piezoelectrics sensors connected to shunt circuits. One uses the SEM for the numerical implementation. The results illustrate the rainbow trap technique, where each shunt was configured to resonate in a determined frequency, where the energy was satisfactorily dissipated at each shunt frequency. A significant attenuation was achieved when all shunts were active simultaneously showing the efficiency of strategy for tunable broadband vibration control and attenuation.

Authorship statement. The authors hereby confirm that they are the sole liable persons responsible for the authorship of this work, and that all material that has been herein included as part of the present paper is either the property (and authorship) of the authors, or has the permission of the owners to be included here.

References

[1] Airoldi, L., and Ruzzene, M., 2011. "Design of tunable acoustic metamaterials through periodic arrays of resonant shunted piezo". New Journal of Physics, 13(11), Nov., p. 113010.
[2] Casadei F, Ruzzene M, Dozio L and Cunefare K A 2010 Smart Mater. Struct. 19 015002
[3] Chen, Y. Y. et al., 2014. "Band gap control in an active elastic metamaterial with negative capacitance piezoelectric shunting". Journal of Vibration and Acoustics, v. 136
[4] Cardella, D., Celli, P., and Gonella S., Manipulating waves by distilling frequencies: a tunable shunt-enabled rainbow trap, Smart Materials and Structures, 25 (2016) 085017 (9pp).
[5] Doyle, J. F., 1997. Wave Propagation in Structures, Springer Verlag, New York.
[6] Hagood N and von Flotow A 1991 J. Sound Vib. 146 243–68
[7] Foward, R. L., 1979. "Electronic damping of vibrations in optical structures". J. Appl.Opt.18(5), p. 690–697.
[8] Lee, U., 2004. Spectral Element Method in Structural Dynamics, Binha University Press.
[9] Leo, D. J., 2007. Engineering analysis of smart material systems. John Wiley and Sons, New Jersey, p. 1–7.
[10] Zhong, W. and Williams, F., 1995. "On the direct solution of wave propagation for repetitive structures". Journal of Sound and Vibration, vol. 181, no. 3, pp. 485-501.
[11] Zhou W, Wu Y and Zuo L 2015 Smart Mater. Struct. 24 065021
[12] Gripp, J. A. B., and Rade, D. A., 2018. "Vibration and noise control using shunted piezoelectric transducers: A review". Mechanical Systems and Signal Processing, 112, Nov., pp. 359–383.
[13] Machado, M. R., Fabro, A. T., and Moura, B. B., 2019. "Spectral element approach for flexural waves control in smart material beam with single and multiple resonant impedance shunt circuit". Journal of Computational and Nonlinear Dynamics.
[14] Moura, B. B. et al., 2020. "Vibration and wave propagation control in a smart metamaterial beam with periodic arrays of shunted piezoelectric pathes". 49th International Congress and Exposition on Noise Control Engineering, INTER-NOISE, Seoul, Korea.
[15] Moura, B. B. and Machado, M. M., 2021. "Vibration control using piezoelectric connected with shunts circuits". 14th World Congress on Computational Mechanics (WCCM), ECCOMAS Congress, Virtual Congress.